

1 **Single Defect Center Scanning Near-Field Optical Microscopy on Graphene**

2

3

4 J. Tisler, T. Oeckinghaus, R. Stöhr, R. Kolesov, F. Reinhard and J. Wrachtrup

5 3. Institute of Physics, Stuttgart University, 70550 Stuttgart, Germany

6

7

8

9 **Abstract**

10 We demonstrate high resolution scanning fluorescence resonance energy transfer
11 microscopy between a single nitrogen-vacancy center as donor and graphene as acceptor.
12 Images with few nanometer resolution of single and multilayer graphene structures were
13 attained. An energy transfer efficiency of 30% at distances of 10nm between a single
14 defect and graphene was measured. Further the energy transfer distance dependence of
15 the nitrogen-vacancy center to graphene was measured to show the predicted d^{-4}
16 dependence. Our studies pave the way towards a diamond defect center based versatile
17 single emitter scanning microscope.

18

19 **Introduction**

20 Imaging the optical near field of nano-sized structures is of fundamental interest to
21 various areas of photonic-, material- and biological sciences.

22 As a result a wealth of scanning near-field optical microscopy (SNOM) techniques are
23 available nowadays ¹. A notable extension to SNOM is scanning fluorescence resonance
24 energy transfer microscopy ². The method exploits fluorescence resonance energy
25 transfer (FRET)³, a non-radiative dipole-dipole interaction between transition dipole
26 moments of a donor and an acceptor. As the method exploits the near field interaction of

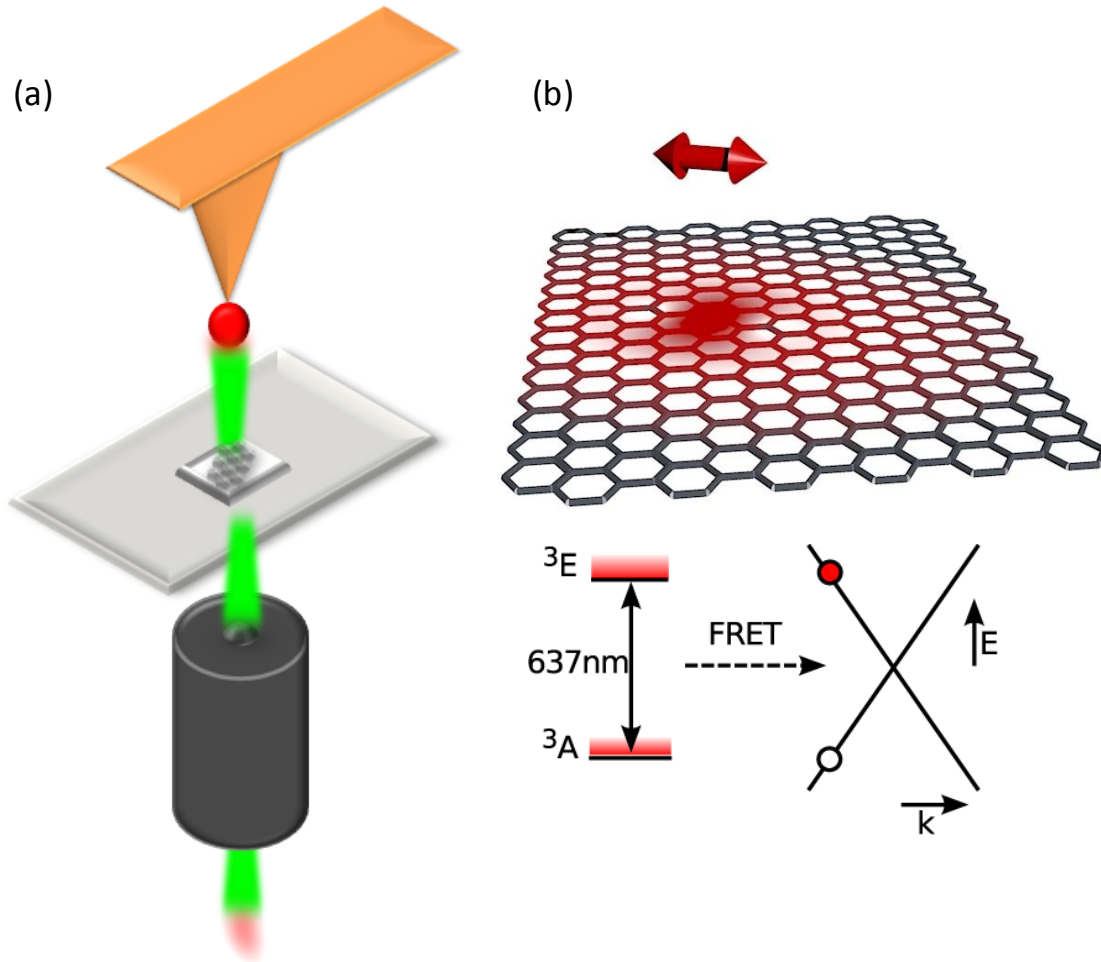
27 two induced dipoles it has a steep dependence on distance d (z^{-6}) and promises to be
28 capable of achieving nm resolution. Different donors and acceptor systems have been
29 used like dyes⁴, color centers⁵ or quantum dots⁶. But most of these systems suffer from
30 blinking or limited photostability rendering their use cumbersome in practice At low
31 temperature single molecular fluorescence usually is stable and as a consequence
32 scanning fluorescence imaging of light fields has been demonstrated ⁷. One particular
33 photoactive system, namely the nitrogen-vacancy (NV) center in diamond has gained
34 attention as an atom-like photon emitter. It proves to be photostable even at room
35 temperature ⁸, can be brought into nm proximity of any photonic system ⁹ and has been
36 proposed as a stable emitter for near-field microscopy⁴. As a result FRET has been
37 demonstrated between a NV and another single molecule with high transfer efficiency
38 ^{10,11}. Therefore it appears to be an ideal emitter for FRET SNOM. In this study we utilize
39 a scanning near field FRET microscope to investigate the interaction of a single NV
40 emitter with graphene. Graphene has a number of intriguing near-field optical properties
41 like high mode density¹² and it is speculated that graphene plasmons are easily launched
42 by near field interactions with emitters. Further on only 2.3% of the incoming far field
43 plane wave absorbed from a monolayer¹³ making near and far field effects to be clearly
44 distinguishable. Owing to its two dimensional geometry the distance dependence of the
45 FRET efficiency is expected to be z^{-4} dependent¹⁴ rather than z^{-6} . Additionally the FRET
46 transfer efficiency probes relevant material properties like the local fermi energy.

47

48

49 **Results**

50 All the experiment use a home-build scanning FRET microscope based on an atomic
 51 force microscope (AFM) with an optically accessible tip. Single NV centers inside
 52 nanodiamonds on the tip of the AFM are used as FRET donors. A laser beam exciting the
 53 NV center is focused through the sample onto the NV. Fluorescence of the defect center
 54 is collected through the same channel (see Fig. 1).



55 **Figure 1: Schematic images of the experiment** (a) Schematic image of the
 56 experimental setup. Nanodiamonds are glued onto the apex of a Si tip. A high
 57 numerical aperture objective (NA 1.3 is used to excite a single NV in the
 58 nanodiamond and collect NV fluorescence. (b) Energy levels of the lowest optical
 59

60 **transition relevant for energy transfer and and graphene band structure near the Γ**
 61 **point.**

62

63 To allow for close proximity between the defect and graphene small nanodiamond with
 64 diameters around $\sim 25\text{nm}$ containing single NV centers were used. When the NV center
 65 is placed in close proximity to the graphene sample, its fluorescence is quenched by
 66 Förster energy transfer. In this process, an electronic excitation of the NV center is
 67 nonradiatively transferred into an exciton in graphene (Fig. 1b) which quickly dissipates
 68 excitation energy mostly by internal radiationless decay¹⁵ occurring at a rate γ_{nr} , this
 69 process competes with radiative emission of the NV center and reduces the fluorescence
 70 intensity to a value

$$I = \frac{\gamma_{ex}\gamma_r}{\gamma_r + \gamma_{nr}}$$

71 where γ_{ex} and γ_r are the excitation rate and radiative rate, respectively, and we assume
 72 γ_{ex} to be much below saturation.

73 The quenching rate γ_{nr} can be computed from Förster's law¹⁶ with the additional
 74 assumption that a sheet of graphene can be approximated by a two-dimensional array of
 75 infinitesimal flakes¹⁷.

$$\gamma_{nr} = A \iint_{\text{graphene sheet}} ds^2 |\mathbf{E}_p|^2 \mu_g^2 = A \iint_{\text{graphene sheet}} ds^2 \frac{\mu_{eg}^2 \mu_g^2 f(\hat{\mathbf{r}}, \widehat{\boldsymbol{\mu}}_{eg})}{r^6} \quad (1).$$

76 Here, A is a proportionality constant and $\mathbf{E}_p = \mathbf{E} - (\mathbf{e}_z \cdot \mathbf{E})\mathbf{e}_z$ denotes the in-plane
 77 component of $\mathbf{E} = (3\hat{\mathbf{r}}(\boldsymbol{\mu}_{eg} \cdot \hat{\mathbf{r}}) - \boldsymbol{\mu}_{eg})/(4\pi\epsilon_0 r^3)$, the near-field of the transition
 78 dipole $\boldsymbol{\mu}_{eg} = -e\langle e|\mathbf{r}|g\rangle$ of the NV center's optical transition between states $|g\rangle$ and $|e\rangle$
 79 (red shade in Fig. 1b). The graphene transition dipole moment μ_g is a scalar, reflecting the

80 fact that graphene is an isotropic material. Hence, exciton transitions can be driven by
 81 any in-plane driving field $\mathbf{E}_p = E \mathbf{e}_p$, regardless of its polarization \mathbf{e}_p . Precisely,
 82 $ds^2 \mu_g^2 = e^2 \sum_{\mathbf{k}_i, \mathbf{k}_f, \omega=v_F(\mathbf{k}_f + \mathbf{k}_i)} |\langle \mathbf{k}_f | x | \mathbf{k}_i \rangle|^2$ where $|\mathbf{k}_i\rangle, |\mathbf{k}_f\rangle$ denote plane-wave
 83 electron states in graphene and ω is the NV transition's frequency.
 84 Integrating equation (1) over an infinitely large graphene surface yields a modified
 85 Förster type law

$$\gamma_{nr} = \gamma_r \frac{z_0^4}{z^4}, \quad (2)$$

86 with a Förster distance z_0 and a quenching rate rising with the fourth power of distance,
 87 differing markedly from the z^{-6} law commonly known for point like objects such as
 88 molecules or atoms.

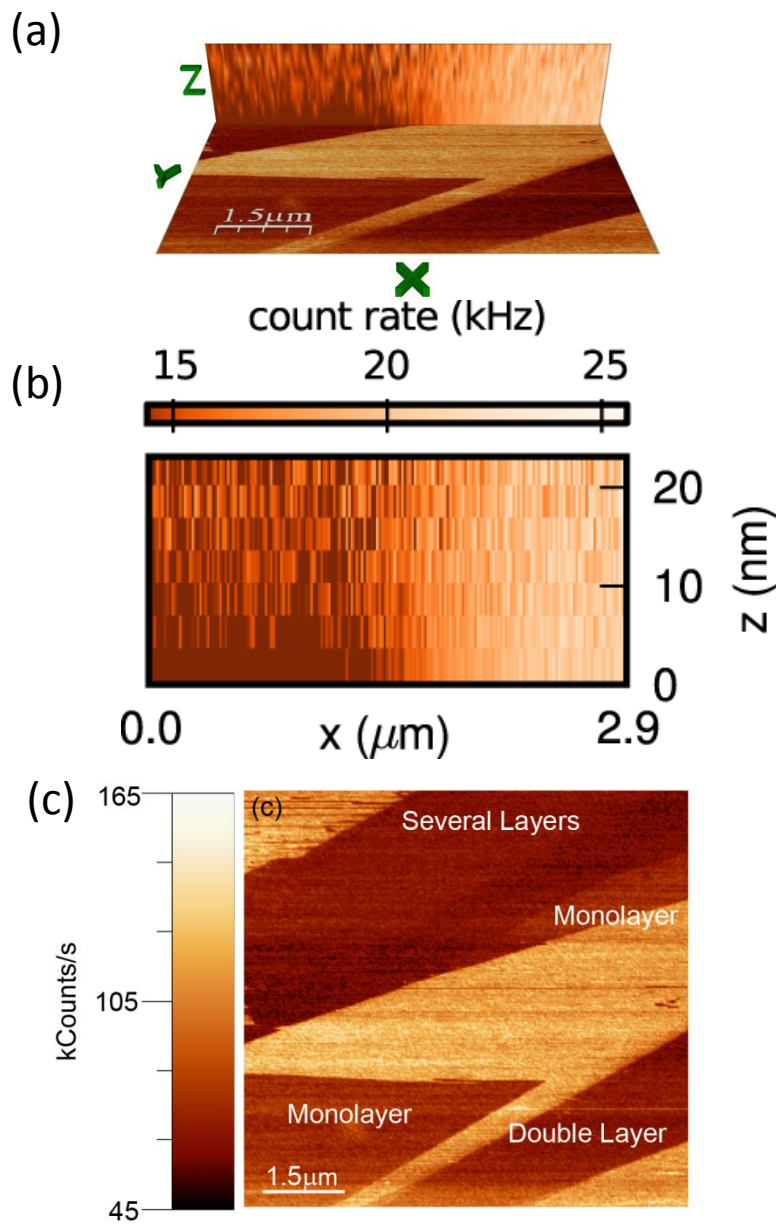
89 Quantitatively, the Förster distance can be calculated from eq. (2) and the expressions of
 90 γ_{nr} and γ_r stated in previous work^{7,14}.

$$91 \quad z_0 = \sqrt[4]{\frac{9e^2 \hbar^3 c^3}{4 \cdot 512 (\hbar \omega)^4 \epsilon_0}} = 15.3 \text{nm}. \quad (3)$$

92

93

94



95

96

97 **Figure 2: Scanning FRET on graphene mono- and multiple layers. Plots show the**
 98 **NV fluorescence intensity as a function of lateral (c) as well as lateral and axial**
 99 **position over the graphene sample.**

100 In the following we discuss our scanning FRET experiments on layers of different

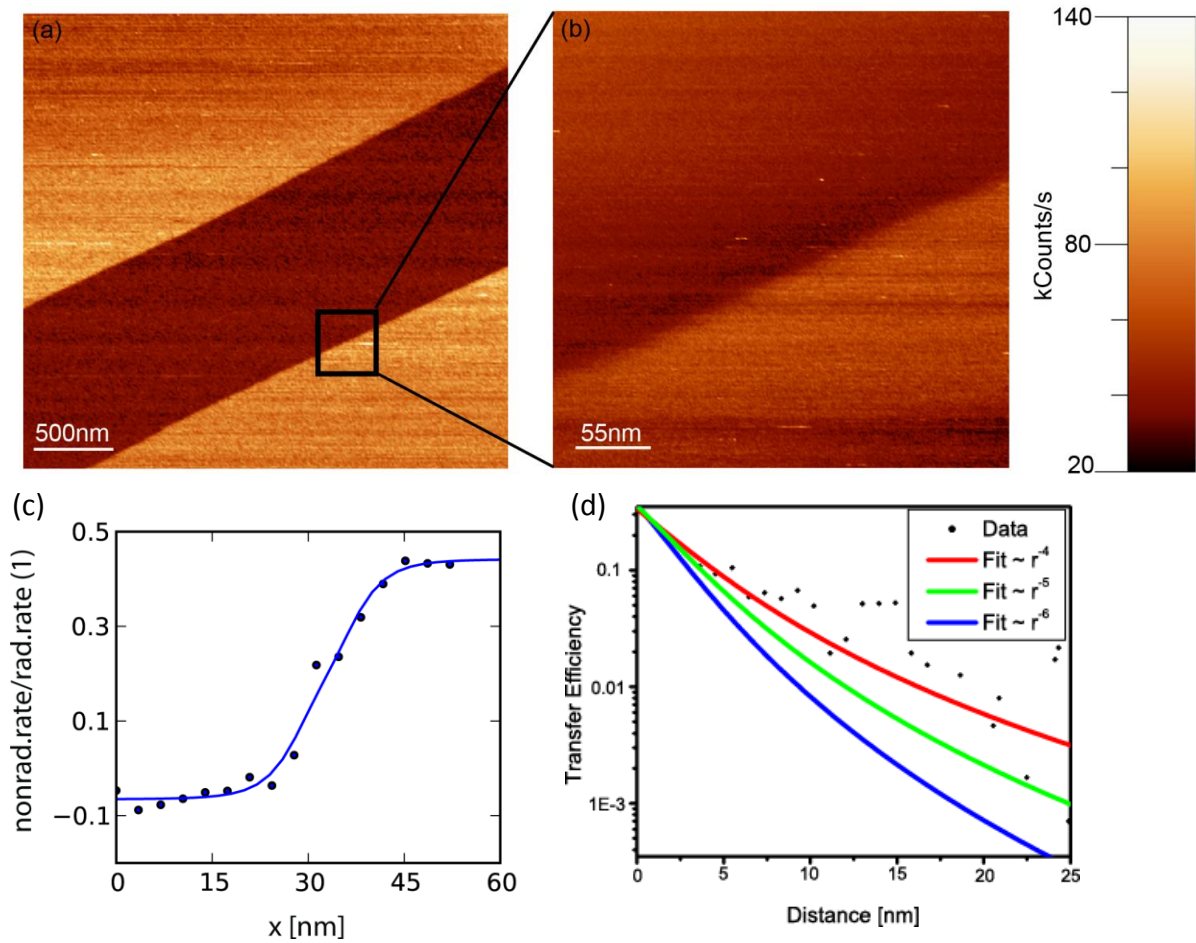
101 graphene thickness. It is worth mentioning that in addition to lateral xy scans we also

102 measured in xz- and in xy-direction. For such images tapping mode scanning FRET is
103 used. In this mode the tip of the AFM is oscillating during scanning in contrast to contact
104 mode. The photons arriving during the scan are measured in registry with the different
105 heights of the oscillating tip.. Fig. 2b shows a corresponding image in the xz plane. To
106 compare eq. (1) with results from Fig. 2c, we transform the fluorescence
107 $I(x, y, z)$ observed in measurements into a quenching rate $\gamma_{nr}(x, y, z)$ by the relation

$$108 \quad \gamma_{nr} = \left(\frac{I_0}{I(x,y,z)} - 1 \right) \gamma_r, \quad (4)$$

109 where I_0 is the unquenched NV fluorescence intensity. In all the following, we assume a
110 radiative rate $\gamma_r = 1/\tau_{NV}$ based on the measured fluorescence lifetime $\tau_{NV} = 13\text{ns}^{18}$.
111 Note that this conversion implicitly assumes unity quantum efficiency.

112 In case of Fig. 2 the monolayer quenching rate was $27.7\text{E}^6 \text{ s}^{-1}$ for a double layer $33.1\text{E}^6 \text{ s}^{-1}$
113 and for several layers $46.2\text{E}^6 \text{ s}^{-1}$. In contrast to previous work¹⁹ no exact scaling with
114 layer thickness was observed, probably due to background contributions which were not
115 taken into account in our measurements.



116

117 **Figure 3: Quantitative comparison of scanning fluorescence resonance energy**

118 **transfer microscopy images to theory. A high resolution contact-mode scan of a**

119 **graphene edge (a-b) is used to measure the step response function of the single NV**

120 **center scanning over the graphene monolayer (c) The solid line of (c) is a fit to the**

121 **data using eq. (1), parametrized by the NV-graphene distance of $z_{NV} = 9.8$ nm. (d)**

122 **Vertical dependence $\gamma_{NV}(z)$. A fit of the data (red line) agrees with the predicted**

123 **z^{-4} law (eq. (2)) for a Förster distance of $z_0 = 8.25 \pm 0.13$ nm.**

124

125 Thanks to their atomic size, scanning single emitters are able to map near-field couplings

126 with molecular (nm) resolution in all three dimensions. As a first application of this

127 remarkable property, we experimentally confirmed the theoretical model of eq. (1). The
 128 result is shown in Fig. 3. In the lateral dimensions (Fig. 3 a-c), a high-resolution scan of a
 129 graphene edge (Fig. 3b) reveals that fluorescence drops smoothly over a length scale of
 130 $\sim 10\text{nm}$ when the NV center is moved over the flake. The theoretical prediction (solid line
 131 in Fig. 3c) is obtained by numerically integrating equation (1), taking into account the
 132 fact that the NV transition has two orthogonal transition dipoles $\boldsymbol{\mu}_1, \boldsymbol{\mu}_2$

$$\gamma_{nr}(x) = \left(\gamma_{nr}^{\mu_1}(x) + \gamma_{nr}^{\mu_2}(x) \right) / 2$$

$$\gamma_{nr}^{\mu}(x) = A\mu_g^2 \int_x^{\infty} dx \int_{-\infty}^{\infty} dy \left| \mathbf{E}_p^{z_{NV}, \mu}(x, y) \right|^2.$$

133 The remaining free parameters A, μ_g^2 and z_{NV} are fit to the data and the dipole
 134 orientation is chosen as $\boldsymbol{\mu}_1 \parallel \mathbf{e}_z, \boldsymbol{\mu}_2 \parallel \mathbf{e}_x$ to best fit the observed behaviour. We find that
 135 the data agrees well with the theoretical prediction (Fig. 3c). The achieved resolution is
 136 limited by the spatial extent of the near-field \mathbf{E}_p , which is of the order of the NV-
 137 graphene distance. Reverting the argument, we can extract this distance from the fit,
 138 finding that $z_{NV} = 9.8 \text{ nm}$. This value is nonzero even though the nanodiamond was
 139 scanned over the graphene in contact mode. Therefore, we interpret this value as the
 140 distance between the NV center and the surface of the nanodiamond.

141 We also measured the vertical dependence $\gamma_{nr}(z)$ by repeatedly approaching and
 142 retracting the tip on a large graphene surface (Fig 3d). Again, we find that the data is well
 143 described by eq. (1) and in particular agrees with the predicted z^{-4} law of eq. (2). Using
 144 the value z_{NV} obtained from the lateral scan, we can quantitatively fit the data and infer a
 145 Förster distance of $z_0 = 8.25 \pm 0.13 \text{ nm}$. This differs significantly from the theory
 146 prediction ($z_0 = 15.3\text{nm}$, eq. (3)). Most likely, this difference is due to additional

147 nonradiative channels which lower the NV center's quantum efficiency and thus reduce
148 z_0 . The existence of such channels is likely and candidates include quenching by the
149 silicon AFM tip or an intrinsically low quantum efficiency in nanodiamonds. Conversely,
150 we note that our result provides a method to measure the quantum efficiency of a single
151 emitter when it is combined with a quantitative theory of excitonic transitions in
152 graphene¹⁴²⁰.

153

154 **Conclusion**

155 We demonstrated optical scanning fluorescence resonance energy transfer microscopy
156 with a single NV center in nanodiamond as emitter. By scanning over a graphene
157 monolayer we attained nanometer resolution images and a transfer efficiency as large as
158 30%. Furthermore we experimentally confirmed a z^{-4} dependence of the energy transfer
159 rate between a point-like emitter and a graphene monolayer. While graphene is an
160 interesting photonic material in its own right, application of the technique to other nano
161 photonic structures and acceptors, e.g. single molecules certainly would be of great
162 interest. Applications in biological sciences where scanning FRET might become a
163 valuable addition to other FRET based techniques for, e.g. imaging larger protein
164 structures of cellular surfaces are easily envisioned. Such methods may be combined with
165 the magnetic field sensing capabilities of the NV center to yield a truly multifunctional
166 local probe.

167

168

169 Acknowledgement

170 Financial support by the EU via projects SQUTEC and DINAMO as well as the German

171 Science foundation via research group 1493 and SFB/TR 21 is acknowledged.

172

173 References

- 174 1. Betzig, E., Trautman, J. K., Harris, T. D., Weiner, J. S. & Kostelak, R. L. Breaking
175 the Diffraction Barrier: Optical Microscopy on a Nanometric Scale. *Science* **251**,
176 1468–1470 (1991).
- 177 2. Sekatskii, S. K. & Letokhov, V. S. Nanometer-resolution scanning optical
178 microscope with resonance excitation of the fluorescence of the samples from a
179 single-atom excited center. *Jetp Lett.* **63**, 319–323 (1996).
- 180 3. Lakowicz, J. R. *Principles of fluorescence spectroscopy*. (Springer: 2006).
- 181 4. Gruber, A. *et al.* Scanning Confocal Optical Microscopy and Magnetic Resonance on
182 Single Defect Centers. *Science* **276**, 2012–2014 (1997).
- 183 5. Shubeita, G. T. *et al.* Scanning near-field optical microscopy using semiconductor
184 nanocrystals as a local fluorescence and fluorescence resonance energy transfer
185 source. *J Microsc* **210**, 274–278 (2003).
- 186 6. Y. Ebenstein, T. M. Quantum-Dot-Functionalized Scanning Probes for Fluorescence-
187 Energy-Transfer-Based Microscopy. (2003).doi:10.1021/jp036135j
- 188 7. Michaelis, J. *et al.* A single molecule as a probe of optical intensity distribution. *Opt.*
189 *Lett.* **24**, 581–583 (1999).
- 190 8. Michalet, X. *et al.* Quantum Dots for Live Cells, in Vivo Imaging, and Diagnostics.
191 *Science* **307**, 538–544 (2005).
- 192 9. Kurtsiefer, C., Mayer, S., Zarda, P. & Weinfurter, H. Stable Solid-State Source of
193 Single Photons. *Phys. Rev. Lett.* **85**, 290–293 (2000).
- 194 10. Tisler, J. *et al.* Highly Efficient FRET from a Single Nitrogen-Vacancy Center in
195 Nanodiamonds to a Single Organic Molecule. *ACS Nano* **5**, 7893–7898 (2011).
- 196 11. Kühn, S., Hettich, C., Schmitt, C., Poizat, J.-P. & Sandoghdar, V. Diamond colour
197 centres as a nanoscopic light source for scanning near-field optical microscopy.
198 *Journal of Microscopy* **202**, 2–6 (2001).
- 199 12. Koppens, F. H. L., Chang, D. E. & García de Abajo, F. J. Graphene Plasmonics: A
200 Platform for Strong Light-Matter Interactions. *Nano Letters* (2011).at
201 <<http://resolver.caltech.edu/CaltechAUTHORS:20110929-105946388>>
- 202 13. Nair, R. R. *et al.* Fine Structure Constant Defines Visual Transparency of Graphene.
203 *Science* **320**, 1308–1308 (2008).
- 204 14. Swathi, R. S. & Sebastian, K. L. Long range resonance energy transfer from a dye
205 molecule to graphene has (distance)⁻⁴ dependence. *The Journal of Chemical Physics*
206 **130**, 086101–086101–3 (2009).

- 207 15. Stöhr, R. J., Kolesov, R., Pflaum, J. & Wrachtrup, J. Fluorescence of laser-created
208 electron-hole plasma in graphene. *Phys. Rev. B* **82**, 121408 (2010).
- 209 16. Förster, T. Zwischenmolekulare Energiewanderung und Fluoreszenz. *Annalen der*
210 *Physik* **437**, 55–75 (1948).
- 211 17. Stöhr, R. J. *et al.* Super-resolution Fluorescence Quenching Microscopy of Graphene.
212 *ACS Nano* **6**, 9175–9181 (2012).
- 213 18. Robledo, L., Bernien, H., Sar, T. van der & Hanson, R. Spin dynamics in the optical
214 cycle of single nitrogen-vacancy centres in diamond. *New Journal of Physics* **13**,
215 025013 (2011).
- 216 19. Chen, Z., Berciaud, S., Nuckolls, C., Heinz, T. F. & Brus, L. E. Energy Transfer from
217 Individual Semiconductor Nanocrystals to Graphene. *ACS Nano* **4**, 2964–2968
218 (2010).
- 219 20. Swathi, R. S. & Sebastian, K. L. Resonance energy transfer from a dye molecule to
220 graphene. *The Journal of Chemical Physics* **129**, 054703 (2008).
- 221
- 222
- 223